Purging viral latency by a bifunctional HSV-vectored therapeutic vaccine in chronically SIV-infected macaques

Ziyu Wen,[1#] Pingchao Li,[2#] Yue Yuan,[1#] Congcong Wang,[1#] Minchao Li,[1] Haohang Wang,[1] Minjuan Shi,[1] Yizi He,[2] Mingting Cui,[1] Ling Chen,[2*] Caijun Sun,[1,3*]

[1]School of Public Health (Shenzhen), Sun Yat-sen University, Guangdong, China; [2]State Key Laboratory of Respiratory Disease, Guangzhou Institutes of Biomedicine and Health (GIBH), Chinese Academy of Sciences, Guangzhou, China; [3]Key Laboratory of Tropical Disease Control (Sun Yat-sen University), Ministry of Education, Guangzhou, China.

#These authors contributed equally to this work.

* For correspondence:

Caijun Sun, suncaijun@mail.sysu.edu.cn (CS);

Ling Chen, chen_ling@gibh.ac.cn (LC)

Abstract

The persistence of latent viral reservoirs remains the major obstacle to eradicating human immunodeficiency virus (HIV). We herein reported that recombinant herpes simplex virus type I (HSV-1) with ICP34.5 deletion could more effectively reactivate HIV latency than its wild-type counterpart. Mechanistically, HSV-ΔICP34.5 promoted the phosphorylation of HSF1 by decreasing the recruitment of protein phosphatase 1 (PP1α), thus effectively binding to the HIV LTR to reactivate the latent reservoirs. In addition, HSV-ΔICP34.5 enhanced the phosphorylation of IKKα/β through the degradation of IκBα, leading to p65 accumulation in the nucleus to elicit NF-κB pathway-dependent reactivation of HIV latency. Then, we constructed the recombinant HSV-ΔICP34.5 expressing simian immunodeficiency virus (SIV) env, gag, or the fusion antigen sPD1-SIVgag as an HIV therapeutic vaccine, aiming to achieve a functional cure by simultaneously reactivating viral latency and eliciting antigen-specific immune responses. Results showed that these constructs effectively elicited SIV-specific immune responses, reactivated SIV latency, and delayed viral rebound after the interruption of antiretroviral therapy (ART) in chronically SIV-infected rhesus macaques. Collectively, these findings provide insights into the rational design of HSV-vectored therapeutic strategies for pursuing an HIV functional cure.

Keywords: HIV, SIV, HSV, therapeutic vaccine, functional cure

Introduction

The epidemic of acquired immunodeficiency syndrome (AIDS), caused by human immunodeficiency virus type I (HIV-1), is still a huge challenge for global public health, with approximately 39 million people living with HIV-1 as of 2022. To date, there is neither a curable drug nor a prophylactic vaccine for clinical use against HIV-1 infections. Antiretroviral therapy (ART) can effectively control HIV-1 replication to an undetectable level, but the termination of ART usually results in prompt viral rebound from latent viral reservoirs (Archin et al., 2014, Looker et al., 2017, Calistri et al., 2003, Heng et al., 1994). Thus, it is of great priority to explore novel strategies for curing HIV latency. The “Shock and Kill” strategy is considered a promising approach for purging HIV-1 reservoirs, involving the activation of latently infected cells to express viral products (Shock), followed by viral cytopathic effects or specific cytolytic T lymphocytes (CTLs) to eliminate the activated cells (Kill) (Wu et al., 2022, Yang et al., 2019, Kim et al., 2018). Numerous latency-reversing agents (LRAs) (Yang et al., 2019, Wu et al., 2022), including methylation inhibitors, histone deacetylase (HADC) inhibitors (Archin et al., 2017, Lehrman et al., 2005), and bromodomain and extra terminal domain (BET) protein inhibitors (Li et al., 2013, Bisgrove et al., 2007), have been identified to reactivate latent HIV-1 in preclinical studies, but there is no ideal LRA available for clinical patients yet.

Herpes simplex virus (HSV), a human herpesvirus, features a 152-kb double-stranded DNA genome encoding over 80 proteins (Poh, 2016). Owing to its distinctive genetic background, high capacity, broad tropism, thermostability, and excellent safety profile, modified HSV variants have found extensive applications

in gene therapy and oncolytic virotherapy. For example, talimogene laherparepvec (T-VEC), an HSV-1 variant with ICP34.5 deletion and GM-CSF insertion, received FDA approval in 2015 for treating malignant melanoma, showcasing notable safety and efficacy in clinical practice. Recombinant HSV-based constructs have also emerged as efficacious gene delivery vectors against infectious diseases. Early studies indicated that prophylactic vaccines based on HSV, expressing simian immunodeficiency virus (SIV) antigens, could elicit robust antigen-specific CTL responses in mice and monkeys, providing enduring and partial protection against pathogenic SIVmac239 challenges (Kaur et al., 2007, Murphy et al., 2000). Moreover, increasing data suggest the crucial role of HIV-specific CTL in controlling viral replication and eliminating potential HIV reservoirs (Collins et al., 2020, Leitman et al., 2017). Significantly, epidemiological research suggests a synergistic effect between HSV and HIV infections, with HSV infection in HIV patients being associated with increased HIV-1 viral load and disease progression (Looker et al., 2017, Calistri et al., 2003, Heng et al., 1994). Some studies have further unveiled the ability of HSV to activate HIV latent reservoirs (Amici et al., 2004, Amici et al., 2001, Pierce et al., 2023). Given the potential of HSV to simultaneously induce antigen-specific immune responses and reactivate latent viral reservoirs, we propose a proof-of-concept strategy to achieve an HIV functional cure using a modified bifunctional HSV-vectored therapeutic vaccine.

Results

The modified HSV-ΔICP34.5-based constructs reactivated HIV latency more efficiently than wild-type HSV counterparts

The J-Lat 10.6 cell line, originating from Jurkat T cells with latent HIV-1 provirus, was infected with wild-type HSV-1 17 strain (HSV-wt) at different multiplicities of infection (MOI) to assess its capability to reactivate HIV latency. Flow cytometry analysis showed that green fluorescent protein (GFP) expression was increased in a dose-dependent manner (*Figure 1A*), and the mRNA levels of HIV-1 LTR, Tat, Gag, Vif, and Vpr were also significantly increased in response to HSV stimulation (*Figure 1B*), demonstrating that the latent HIV provirus can be reactivated to a certain extent by wild-type HSV. In addition, different HSV-1 strains, including HSV-1 Mckrae and HSV-1 F strain, can also reactivate HIV latency (*Figure 1 - figure supplement 1*). Remarkably, we found for the first time that the HSV-1 17 strain with ICP34.5 deletion (HSV-ΔICP34.5) could reactivate HIV latency more efficiently than HSV-wt. Specifically, the mRNA levels of HIV genes (LTR, Tat, Gag, Vpr, Vif) were substantially increased in HSV-ΔICP34.5-infected J-Lat 10.6 cells than in HSV-wt treated cells, although there was a weaker replication ability of HSV-ΔICP34.5 in these cells than that of HSV-wt, as indicated by the mRNA level of HSV UL27 (*Figure 1C and D*). Furthermore, this finding was verified in ACH-2 cells, derived from T cells latently infected with replication-competent HIV-1. A significantly higher level of p24 protein, a key indicator of HIV replication, was found in the HSV-ΔICP34.5-infected ACH-2 cells than in the HSV-wt treated cells

(*Figure 1E*), and the mRNA levels of HIV-1-related genes (LTR, Tat, Gag, Vpr, Vif) were also significantly increased (*Figure 1F*). Subsequently, we generated J-Lat 10.6 cells stably expressing ICP34.5-Flag-Tag (J-Lat 10.6-ICP34.5) using the recombinant lentivirus system and confirmed the expression of the ICP34.5 protein (*Figure 1G*). Our research revealed that HSV-ΔICP34.5 displayed reduced reversal capacity for the latent HIV reservoir in J-Lat 10.6-ICP34.5 cells compared to J-Lat 10.6 cells (*Figure 1G*). Furthermore, in J-Lat 10.6-ICP34.5 cells, the potency of latent reversal agents like phorbol 12-myristate 13-acetate (PMA) and TNF-α was notably reduced when contrasted with J-Lat 10.6 cells (*Figure 1H*). These findings indicate that HSV ICP34.5 can effectively inhibit the reactivation of the HIV latency, and HSV constructs lacking ICP34.5 potentially reactivate HIV latency with high efficiency.

The modified HSV-based constructs effectively reactivated HIV latency by modulating the IKKα/β-NF-κB pathway and PP1-HSF1 pathway

Next, the mechanism of potentially reactivating viral latency by the modified HSV-ΔICP34.5-based constructs was explored. J-Lat10.6 cells were infected with HSV-wt and HSV-ΔICP34.5, and our results showed that HSV-ΔICP34.5 significantly enhanced the phosphorylation of IKKα/β, promoted the degradation of IKBα, and thus led to the accumulation of p65 in the nucleus (*Figure 2A*). NF-κB is a well-known host transcription factor that exists in the form of the NF-κB-IκB complex in resting cells, but IκB can degrade and release the NF-κB dimer to enter the

nucleus and promote gene transcription in response to external stimulation. Using the coimmunoprecipitation (Co-IP) assay, we verified that the ICP34.5 protein had a specific interaction with IKKα/β, and then ICP34.5 could dephosphorylate IKKα/β. Moreover, the overexpression of ICP34.5 effectively inhibited lipopolysaccharide (LPS) -induced NF-κB pathway activation by inhibiting p65 entry into the nucleus (*Figure 2B-C*).

To further clarify the underlying mechanism, we next performed the IP-MS assay to identify other potential molecules contributing to this reactivation in J-Lat 10.6-ICP34.5 overexpressing cells, and we found that ICP34.5 can also interact with heat shock 1 protein (HSF1) (*table supplement* 1). HSF1 has been reported as a transcription factor correlated with the reactivation of HIV latency (Xu et al., 2022, Lin et al., 2018, Zeng et al., 2017). To test whether HSF1 contributes to the reactivation of HIV latency by HSV-ΔICP34.5-based constructs, KRIBB11, an inhibitor of HSF1, was administered to HSV-ΔICP34.5-infected J-Lat 10.6 cells. The results indicated that the reactivation ability of HSV-ΔICP34.5 was significantly inhibited by KRIBB11 treatment in a dose-dependent manner (*Figure 2D and E*). Furthermore, a significant enhancement of the binding of HSF1 to the HIV LTR was observed upon HSV-ΔICP34.5 infection, leading to an increase in the reactivation of HIV latency (*Figure 2F*). The direct interaction between ICP34.5 and HSF1 was also identified by Co-IP assay. Importantly, HSF1 was effectively dephosphorylated at Ser320 as a result of the overexpression of ICP34.5, while no influence on the mRNA or protein expression of HSF1 was observed (*Figure 2, G and H, Figure 2-figure supplement 2*). Considering that protein phosphatase 1

(PP1) can interact with ICP34.5 and dephosphorylate eIF2α (Li et al., 2011), we then investigated the interaction between PP1α and ICP34.5 (*Figure 2I*). Additionally, a direct interaction between PP1α and HSF1 was found (*Figure 2J-L*), allowing for the dephosphorylation of HSF1 and then affecting its ability to reactivate HIV latency.

Collectively, these findings demonstrated that our modified HSV-ΔICP34.5-based constructs effectively reactivated HIV latency by modulating the IKKα/β-NF-κB pathway and PP1-HSF1 pathway.

Construction of recombinant HSV-1 expressing exogenous SIV genes elicited robust immune responses in mice

Prior research suggested that HSV-ΔICP34.5 holds significant promise in reactivating latent HIV efficiently. Subsequently, we explored the potential of advancing HSV-ΔICP34.5 as a bifunctional therapeutic vector to revive latent viral reservoirs and inducing antigen-specific immune responses against chronic HIV infection. To achieve this, the HSV-1 ICP34.5 gene was selectively knocked out, and exogenous antigens were introduced using the bacterial artificial chromosome (BAC)/galactokinase (galK) selection system. Additionally, the ICP47 gene was ablated to augment the immunogenicity of the HSV vector (*Figure 3A, Figure 3-figure supplement 3*). A series of recombinant HSV-ΔICP34.5ΔICP47-based vectors expressing SIV gag and env antigen were constructed, and the antigen expression of these constructs was confirmed by Western blotting assay (*Figure 3B and C*). Furthermore, to improve the immunogenicity of the targeted antigen,

we fused the SIV gag with soluble PD1 (sPD1), enabling it to competitively bind with PD-L1 and thereby block the PD1/PD-L1 immune inhibitory pathway (*Figure 3D*). Consistent with the above findings, these HSV-ΔICP34.5ΔICP47-based SIV vaccines also efficiently reactivated latent HIV proviruses (*Figure 3-figure supplement 4*). Then, the immunogenicity of the above modified HSV-ΔICP34.5ΔICP47-based SIV vaccine was assessed in mice (*Figure 3E*). Our results showed that these constructs effectively elicited SIV antigen-specific T cell immune responses using the interferon γ (IFN-γ) ELISpot assay and the intracellular cytokine staining (ICS) assay (*Figure 3F-M*). Of note, the frequency of SIV Gag-specific IFN-γ -secreting spot-forming cells (SFCs) in the HSV-sPD1-SIVgag group (1350 SFCs per 10^6 splenocytes) was significantly higher than that in the HSV-SIVgag group (498 SFCs per 10^6 splenocytes) (*Figure 3F*). The frequency of SIV Env2-specific IFN-γ -secreting SFCs in the HSV- SIVenv group was significantly higher than the HSV-empty group (*Figure 3G*). Furthermore, the functionality of antigen-specific T cell subsets in response to SIV antigen stimulation was confirmed using the ICS assay (*Figure 3H-M*). Consistently, the HSV-sPD1-SIVgag group showed a significantly higher frequency of SIV-specific $CD3^+$ T, $CD4^+$ T, and $CD8^+$ T cell subsets secreting IFN-γ, IL-2, and TNF-α cytokines compared to the HSV-SIVgag group (*Figure 3I-K*). Notably, a heightened proportion of Gag-specific effector memory T cells (Tem) of $CD8^+$ T cell subset was observed in comparison to the HSV-Gag group (*Figure 3L*). In addition, a higher frequency of SIV- Env2-specific $CD4^+$ T cells secreting IFN-γ was observed in the HSV-SIVenv group than in the HSV-empty group (*Figure 3M*). These data

indicated that the vaccines constructed in this study elicit a T cell immune response in mice. Moreover, the blockade of PD1/PDL1 signaling pathway effectively enhanced vaccine-induced T cell immune responses, which was consistent with our and other previous studies (Zhou et al., 2013, Wu et al., 2022, Pan et al., 2018, Xiao et al., 2014).

The modified HSV-based constructs efficiently elicited SIV-specific immune responses in chronically SIV-infected macaques

Next, the immunogenicity of these HSV-vectored SIV vaccines was further investigated in chronically SIV_{mac239}-infected rhesus macaques (RMs). To mimic chronically infected HIV patients in clinic practice, all RMs used in this study were chronically infected with SIV and received ART treatment for several years, as reported in our previous studies (Pan et al., 2018, Yang et al., 2019, Wu et al., 2021, Wu et al., 2022, He et al., 2023). Based on sex, age, viral load, and CD4 count, nine RMs were assigned into three groups: ART+saline group (n=3), ART+HSV-empty group (n=3), and ART+HSV-sPD1-SIVgag/SIVenv group (n=3). All RMs received ART (FTC/6.7 mg/kg/once daily, PMPA/10 mg/kg/once daily) treatment to avoid the interference of free SIV particles. On day 33 and day 52, these RMs were immunized with saline, HSV-empty, or HSV-sPD1-SIVgag/SIVenv respectively. On day 70, ART treatment in all RMs was discontinued to evaluate the time interval of viral rebound. Samples were collected at different time points to monitor virological and immunological parameters (Figure 4A, *table supplement* 2). To reduce the impact of individual RM variations, the difference in SIV-specific IFN-γ-secreting SFCs between post-immunization and

pre-immunization (ΔSFCs) was used to evaluate the immune response induced by HSV-vectored SIV vaccines. The results showed that SIV Gag-specific ΔSFCs in the ART+HSV-sPD1-SIVgag/SIVenv group were greatly increased when compared with those in the ART+HSV-empty group and ART+saline group (*Figure 4B-D*). A similar enhancement of SIV Gag-specific TNF-α -secreting $CD4^+$ T and $CD8^+$ T subsets was also verified by ICS assay (*Figure 4E*). Collectively, these data demonstrated that the HSV-sPD1-SIVgag/SIVenv construct elicited robust SIV-specific T cell immune responses in ART-treated, SIV-infected RMs.

The modified HSV-based constructs effectively reactivated SIV latency in vivo and delayed viral rebound in chronically SIV-infected, ART-treated macaques

Finally, we investigated the therapeutic efficacy of HSV-sPD1-SIVgag/SIVenv in chronically SIV-infected, ART-treated RMs. Consistent with our previous studies, the plasma viral load (VL) in these RMs was effectively suppressed during ART treatment, but rebounded after ART discontinuation. The VL in the ART+saline group promptly rebounded after ART discontinuation, with an average 8.63-fold increase in the rebounded peak VL compared with the pre-ART VL (*Figure 5A, D and E*). However, plasma VL in the ART+HSV-empty group and the ART+HSV-sPD1-SIVgag/SIVenv group exhibited a delayed rebound interval (*Figure 5B-D*). Remarkably, there was a lower rebounded peak VL than pre-ART VL in the ART+HSV-sPD1-SIVgag/SIVenv group (average 12.20-fold decrease), while a higher rebounded peak VL than pre-ART VL in the ART+HSV-empty group

(average 2.74-fold increase) (*Figure 5E*). Then, we assessed the potential effect on the latent SIV reservoirs in vivo by administering our modified HSV-based SIV therapeutic constructs in these RMs. Although there were no obvious viral blips observed in these RMs, we found significant suppression of integrated SIV DNA provirus in the ART+HSV-sPD1-SIVgag/SIVenv group. However, the copies of the SIV DNA provirus were significantly improved in the ART+HSV-empty group and ART+saline group (*Figure 5F*). More interestingly, we next assessed the magnitude of SIV Pol antigen-specific immune responses, which could represent to some extent the level of newly generated virions from the reactivated SIV reservoirs, because SIV Pol antigen was not included in our designed vaccine constructs. Specifically, the Pol-specific SFCs amount on Day 70 (511 SFCs/10^6 PBMCs, post-vaccination) was higher than that on Day 33 (315 SFCs/10^6 PBMCs, pre-vaccination) in the ART+HSV-sPD1-SIVgag/SIVenv group. In addition, there was a similar observation in the ART+HSV-empty group. In contrast, the Pol-specific SFCs gradually decreased with the duration of ART treatment in the ART+saline group (*Figure 5G*). In addition, the $CD4^+$ /$CD8^+$ T cell ratio (*Figure 5H*) and body weight (*Figure 5-figure supplement 5*) after treatment were effectively ameliorated in the RMs of the ART+HSV-sPD1-SIVgag/SIVenv group, but not in the ART+HSV-empty group and ART+saline group. Taken together, these findings suggested that the latent SIV reservoirs might be effectively purged because of the effect of simultaneously reactivating viral latency and eliciting SIV-specific immune responses by our modified HSV-based SIV therapeutic constructs, thus resulting in a delayed viral rebound in chronically SIV-infected, ART-treated macaques.

Discussion

To conquer the continuous epidemic of AIDS, exploring novel strategies to render and eliminate HIV latency should stand as a pivotal pursuit. Currently, numerous strategies, including shock and kill, block and lock, chimeric antigen receptor T-cell therapy, therapeutic vaccination, and gene editing, have been extensively investigated to target the latent HIV reservoirs for an HIV functional cure (Deeks, 2012, Yeh and Ho, 2021, Maldini et al., 2020, Herzig et al., 2019, Dash et al., 2023, Dashti et al., 2023, Walker-Sperling et al., 2022). However, there is no safe and effective approach for clinical use in HIV-1 patients yet. In the present study, we occasionally found that the modified HSV-ΔICP34.5-based constructs could reactivate HIV latency more efficiently than wild-type HSV counterpart, which inspired us to develop a proof-of-concept strategy based on a bifunctional HSV-vectored therapeutic vaccine, aiming to simultaneously reactivate viral latency and elicit HIV/SIV-specific immune responses for HIV functional cure. Our results indicated that these modified HSV-based constructs efficiently elicited antigen-specific immune responses in mice and chronically SIV-infected macaques, and further therapeutic efficacy experiments showed that this strategy effectively reactivated SIV latency in vivo and delayed viral rebound in chronically SIV-infected, ART-treated macaques (*Figure 6*).

The latent HIV proviruses can harbor it into the host genome with a quiescent transcription state, and thus cannot be recognized by immune surveillance or drug killing (Churchill et al., 2016, Pierson et al., 2000). Therefore, it is critical to disrupt viral latency for developing an HIV cure strategy. Based on our experimental data,

the mechanism for efficiently reactivating viral latency by the modified HSV-ΔICP34.5-based constructs may involve regulating the IKKα/β-NF-κB pathway and PP1-HSF1 pathway. Indeed, during its replication, HSV can activate the double-stranded RNA-dependent protein kinase (PKR) pathway, and thus phosphorylate the protein translation initiation regulator eIF2α, resulting in the initiation of protein translation (Farassati et al., 2001). Previous studies have shown that the reactivation potential of HSV might be intertwined with NF-κB, Sp1, and other unknown transcription factors by ICP0, ICP4, and ICP27 (Chapman et al., 1991, Amici et al., 2004, Vlach and Pitha, 1992, Mosca et al., 1987b, Golden et al., 1992, Vlach and Pitha, 1993, Mosca et al., 1987a). However, the underlying mechanism by which the ICP34.5-deleted HSV construct can greatly improve the reactivation efficacy of HIV latency remains elusive. ICP34.5 is a neurotoxic factor that can antagonize innate immune responses, including PKR, TANK binding kinase (TBK1) signaling, and Beclin1-mediated apoptosis (He et al., 1997, Manivanh et al., 2017, Orvedahl et al., 2007). ICP34.5 binds to host PP1 and mediates the dephosphorylation of eIF2α, thus allowing protein synthesis and reversing the effects of PKR and host antiviral functions (He et al., 1997, He et al., 1998). In this study, our findings further unveiled an interaction between ICP34.5 and HSF1, resulting in reduced HSF1 phosphorylation via recruitment of PP1α. Interestingly, previous reports indicated that HSF1 could positively regulate HIV gene transcription (Rawat and Mitra, 2011), which is facilitated by its nuclear entry post-phosphorylation and subsequent recruitment of p300 for self-acetylation, along with binding to the HIV-1 LTR. Studies have also shown that HSF1 could further

orchestrate p-TEFb recruitment to promote HIV-1 transcriptional elongation (Peng et al., 2020, Lin et al., 2018, Pan et al., 2016b, Pan et al., 2016a). Under stress-induced conditions, phosphorylation triggers the formation of the HSF1 trimer, thus facilitating its nuclear entry to bind to heat shock elements (HSEs) for gene transcription regulation (Bonner et al., 2000, Timmons et al., 2020). Additionally, we also demonstrated that ICP34.5 interacted with IKKα and IKKβ, thereby impeding NF-κB nuclear entry and further curbing HIV latency. Consistently, previous studies have also suggested that ICP34.5 could disrupt the NF-κB pathway and possibly affect the maturation of dendritic cells (Jin et al., 2011). Intriguingly, these findings collectively indicated that ICP34.5 might play an antagonistic role with the reactivation potential of HSV, and thus our modified HSV-ΔICP34.5 constructs reactivate HIV/SIV latency through the release of imprisonment from ICP34.5.

Another observation in this study is that the HSV-sPD1-SIVgag/SIVenv construct elicited robust and persistent SIV-specific T cell immune responses in ART-treated, chronically SIV-infected macaques. Increasing evidence has indicated that HIV-specific cytolytic T lymphocytes (CTLs) can facilitate the suppression of latent viral reservoirs, and thus, the induction of robust and persistent HIV-specific CTL responses is essential for achieving long-term disease-free and transmission-free HIV control (Collins et al., 2020). Featured polyfunctional $CD8^+$ T cells may contribute to HIV elite controllers or long-term non-progressors, a rare proportion of HIV-infected individuals who can spontaneously control viral replication even without ART treatment (Owen et al.,

2010, Ferre et al., 2009, O'Connell et al., 2009). In addition, both our previous study and others have demonstrated that strong antigen-specific $CD8^+$ T cell immune responses, especially effector memory $CD8^+$ T cells, were associated with a lower viral load, and in vivo $CD8^+$ lymphocyte depletion with intravenous infusion of anti-CD8 monoclonal antibody could lead to dramatical viral rebound in these vaccinated elite macaques (Perdomo-Celis et al., 2022, Pandrea et al., 2011). Notably, previous studies have shown that HSV-based vaccines expressing HIV/SIV antigen did elicit specific $CD8^+$ T cell immune responses in mice and macaques, but the magnitude was not as strong as other viral vectors (Parker et al., 2007, Murphy et al., 2000, Kaur et al., 2007). Therefore, to further improve its immunogenicity in vivo, some modifications were adopted to optimize the HSV-vectored vaccine. 1) The ICP47 protein, encoded by the US12 gene, can bind to the transporter associated with antigen presentation (TAP) 1/2, inhibiting the transport of viral peptides into the endoplasmic reticulum and the loading of peptides onto nascent major histocompatibility complex (MHC) class I molecules to activate $CD8^+$ T cells (Orr et al., 2005). Therefore, the ICP47 gene was deleted from our developed HSV vector. 2) Negative immunoregulatory molecules, including PD1, TIM-3, and LAG-3, are usually involved in the pathogenesis of HIV infection, as well as in chronically SIV-infected macaques. Among them, PD1 upregulation can result in the exhaustion and dysfunction of $CD8^+$ T cells (Trautmann et al., 2006). In addition, PD1 expression on memory $CD4^+$ T cells might be linked with HIV latency. In this study, we modified the SIV antigen by fusing to soluble PD1 (sPD1), which can block the PD1/PDL1 pathway by

competitively binding with PDL1 and thus improve HIV/SIV vaccine-induced $CD8^+$ T cell immune responses (Zhou et al., 2013, Wu et al., 2022, Pan et al., 2018, Xiao et al., 2014).

Although promising, there are still some limitations to our study. First, this is a pilot study with relatively small numbers of RMs, and future studies with a larger number of animals can be conducted to better verify our strategy. Second, the HSV-sPD1-SIVgag/SIVenv vaccine resulted in delayed viral rebound and a lower peak viral load post-rebound than pre-ART treatment but did not completely suppress SIV virus rebound in this study, which may be attributed to suboptimal doses and treatment, implying that we should further optimize this regimen for eventually achieving an HIV functional cure in future studies. Taken together, these findings demonstrated that our modified HSV-ΔICP34.5-based constructs potentially reactivated HIV/SIV latency by modulating the IKKα/β-NF-κB pathway and PP1-HSF1 pathway, and thereby we developed a proof-of-concept HIV functional cure strategy based on a bifunctional HSV-vectored therapeutic vaccine, which can provide insights into the rational design of novel strategies for pursuing an HIV functional cure.

Methods

Mouse ethics statement and vaccination

Female BALB/c mice, aged six to eight weeks, were procured from the Experimental Animal Center of Sun Yat-sen University. A total of twenty-five mice were randomly divided into five groups to evaluate the immunogenicity of the recombinant HSV-vector-based SIV vaccine. During the initial week, each mouse was subcutaneously administered a vaccination of 1×10^6 PFU of the respective recombinant HSV-vector vaccines (HSV-empty, HSV-sPD1, HSV-SIVgag, HSV-sPD1-SIVgag, HSV-SIVenv). Following a two-week interval, a booster vaccination was administered via the subcutaneous route using 2×10^6 PFU of recombinant HSV-vector vaccines. The subsequent assessment of the immune response involved ELISpot and intracellular cytokine staining (ICS) assays in accordance with the vaccination schedule.

Ethics statement and vaccination of macaques

A total of 9 chronically SIV_{mac239}-infected rhesus macaques (RMs) were included in this study. All RMs received ART treatment (FTC/6.7 mg/kg/once daily, PMPA/10 mg/kg/once daily) for a duration of 33 days. The RMs were allocated into three groups based on their baseline plasma SIV viral loads (VL): ART + saline (n=3) as the control group, ART+ HSV-empty (n=3) as the sham group, and ART+ HSV-sPD1-SIVgag/SIVenv (n=3) as the vaccinated group. On day 0, all RMs received ART treatment. Once the VL dropped below the limit of detection (1×10^2 copies/mL), the vaccinated group and sham group were primed with a

subcutaneous vaccination of 1×10^7 PFU HSV-sPD1-SIVgag/SIVenv or HSV-empty, respectively, while the control group received an injection of 0.9% saline. After three weeks of the prime vaccination, the vaccinated group and sham group RMs received a subcutaneous booster vaccination of 5×10^7 PFU HSV-sPD1-SIVgag/SIVenv or HSV-empty, respectively. After two weeks of booster vaccination, the ART treatment for all RMs was interrupted. The immune response was evaluated by IFN-γ ELISpot and ICS assays. Plasma viral load was regularly monitored throughout the studied period.

Peptide pools

The peptide pools, encompassing the complete sequences of SIV Gag, Env, and Pol proteins, comprising 15 amino acids with 11 overlaps, were generously provided by the HIV Reagent Program, National Institutes of Health (NIH), USA. Gag pools comprise 125 peptides, while Env and Pol pools are subdivided into Env1 (109 peptides) and Env2 (109 peptides) pools, as well as Pol1 (131 peptides) and Pol2 (132 peptides) pools. These peptide pools were dissolved in dimethyl sulfoxide (DMSO, Sigma) at a concentration of 0.4 mg/ peptide/mL for subsequent immunological assays.

Construction of recombinant HSV

For the generation of recombinant HSV-vector-based vaccines, we implemented modifications at the ICP34.5 loci through homologous recombination within the BAC-HSV-1 system. Specifically, double copies of the ICP34.5 and ICP47 genes were either deleted or inserted into the respective counterparts: sPD1, SIVgag, sPD1-SIVgag, and SIVenv genes. The sPD1-SIVgag gene was created by fusing

the N-terminal region of mouse soluble PD1 (sPD1) with the C-terminal segment of SIVgag, connected by a GGGSGGG linker, which was engineered through overlapping PCR.

IFN-γ ELISpot assay

The IFN-γ- ELISpot assay was conducted in accordance with our previous study (Sun et al., 2010). In the mouse experiment, 2.5×10^5 freshly isolated mouse spleen lymphocytes were simulated with SIV Gag, Env1, and Env2 peptide pools. In the monkey experiment, 2×10^5 peripheral blood mononuclear cells (PBMCs) were seeded and simulated with the SIV Gag, Env, and Pol peptide pools. Mock stimulation utilized DMSO (Sigma), while concanavalin A (ConA, 10 μg/mL) was employed as a positive control. Spot quantification was performed using an ELISpot reader (Mabtech), and peptide-specific spot counts were determined by subtracting the spots from mock stimulation.

Intracellular cytokine staining (ICS)

The ICS assay was performed as described previously (Wu et al., 2022). In the mouse experiment, 2×10^6 freshly isolated mouse spleen lymphocytes were stimulated with SIV Gag, Env1, and Env2 peptide pools. For the monkey experiment, 2×10^6 PBMCs were seeded and simulated with the SIV Gag, Env, and Pol peptide pools. DMSO and PMA (Thermo Scientific) plus ionomycin were used as the mock and positive controls, respectively. Data analysis was performed using FlowJo software (version 10.8.1), and the antibodies used are listed in *table*

supplement 3. The frequencies of cytokines produced from peptide-specific cells were analyzed by subtracting mock stimulation.

SIV viral RNA and DNA copy assays and absolute T cell count

Absolute T cell count and the levels of plasma mRNA and SIV total DNA were quantified as described previously (Wu et al., 2022). Plasma viral RNA copy numbers were determined via SYBR green-based real-time quantitative PCR (Takara), using SIV gag-specific primers (*table supplement 4*). Viral RNA copy numbers were calculated based on the standard curve established using SIV_{mac239} gag standards. The lower limit of detection for this assay was 100 copies/mL of plasma. Total cellular DNA was extracted from approximately 0.5 to 5 million cells using a QIAamp DNA Blood Minikit (Qiagen). PCR assays were performed with 200 ng samples of DNA, and SIV viral DNA was quantified using a pair of primers targeting a conserved region of the SIV gag gene, as previously described. Quantitation was performed by comparing the results to the standard curve of SIV gag copies.

Plasmids, cells, and viruses

pVAX-Myc-PDL1, pVAX-Flag-ICP34.5, pVAX-Myc-HSF1, pVAX-HA-PP1α: full-length mouse PDL1, full-length HSV-1 ICP34.5, and full-length human HSF1 and human PP1α with N or C-terminal Tag were cloned into the pVAX vector. pVAX-empty, pcDNA3.1-IKKα, and pcDNA3.1-IKKβ plasmids were stored in our laboratory. pVAX-empty was used as a mock transfection in our study.

293T cells (from the embryonic kidney of a female human fetus), Vero cells (from the kidney of a female normal adult African green monkey), and Hela cells (from

the cervical cancer cells of an African American woman) were cultured in complete Dulbecco's modified Eagle's medium (DMEM, Gibco) containing 10% fetal bovine serum (FBS, Gibco) and 1% penicillin/streptomycin (Gibco) at 37°C in an atmosphere of 5% CO_2. The J-Lat 10.6 cells (Jurkat cells contain the HIV-1 full-length genome whose Env was frameshifted and inserted with GFP in place of Nef) and the HIV-1 latently infected $CD4^+$ CEM cells ACH-2 (A3.01 cell integrated HIV-1 proviral DNA) were cultured in complete RPIM640 (Gibco) containing 10% FBS and 1% penicillin/streptomycin at 37°C in an atmosphere of 5% CO_2. J-Lat 10.6-ICP34.5 cells were constructed in our laboratory.

The HSV-1 (McKrae) and HSV-1 (F) strains were stored in our laboratory. HSV-1 (17 strain) was rescued from pBAC-GFP-HSV in Vero cells. HSV-ΔICP34.5 was rescued from pBAC-GFP-HSV-ΔICP34.5 (with double copies of ICP34.5 deleted) in Vero cells.

RT-qPCR

RT-qPCR was performed as described in our previous study (Zhao et al., 2022). Data were normalized to β-actin. The primer sequences are listed in Supplemental Table 4. Fold changes in the threshold cycle (Ct) values were calculated using the $2^{-\Delta\Delta Ct}$ method.

Chromatin immunoprecipitation (ChIP) assay

ChIP analysis was conducted using the SimpleChIP Enzymatic Chromatin IP kit (Agarose Beads) (CST), following the manufacturer's instructions. Quantitative real-time PCR was employed for detecting the LTR sequence. The sequences of

primers used in the LTR ChIP are listed in Supplemental Table 4. % Input= 2% × $2^{[(ct)2\% \text{ input sample (ct) IP sample}]}$.

Co-immunoprecipitation (Co-IP)

Cells were harvested and subjected to Co-IP assay, following the protocol outlined in our previous study (Zhao et al., 2022).

Western blotting analysis

Nuclear and cytoplasmic proteins were extracted by kits following the manufacturer's instructions (Beyotime). The Western blotting assay was performed as previously described (Zhao et al., 2022).

Statistical analysis

GraphPad Prism 8.0 (GraphPad Software, San Diego, California) was used for statistical analysis. For intragroup direct comparisons, Student's unpaired two-tailed *t* test was performed to analyze significant differences. For comparisons of multiple groups, one-way ANOVAs were performed. Significance levels are indicated as *$P < 0.05$, ** $P < 0.01$, *** $P < 0.001$, **** $P < 0.0001$.

Study approval

Mice experiment was approved by the Laboratory Animal Ethics Committee guidelines at Sun Yat-sen University (approval number: SYSU-IACUC-2021-000185). Chinese rhesus macaques (Macaca mulatta) were housed at the Landau Animal Experimental Center, Guangdong Landau Biotechnology Co., Ltd. (approval number: N2021101).

Acknowledgements

We appreciate the staff at the Animal Center of GIBH for their excellent technical assistance. We thank all other members of our group for their helpful advice and discussion to improve this project. We also appreciate the NIH AIDS Research and Reference Reagent Program for providing SIV peptide pools.

Additional information

Competing interests

The authors have declared that no conflict of interest exists.

Funding

This project was supported by National Natural Science Foundation of China (81971927, 82271786, 32370171), National Key R&D Program of China (2022YFE0203100, 2021YFC2300103).

Author Contributions

All authors were involved in drafting or critically revising the manuscript for important intellectual content, and all authors approved the final version for publication. CS conceived the project and provided the main funding. CS and LC designed the experiments and reviewed the manuscript. ZW, PL, YY, and CW performed most of the experiments and analyzed the data. ZW, PL, YY, CW, ML, HW, MS, YH, and MC established the animal models and performed animal experiments. ZW and CS interpreted the data and wrote the manuscript.

Additional files

Supplementary files

Figure S1-S5. Table S1-S4.

Data Availability Statement

Source data contain the numerical data used to generate the figures.

References

AMICI, C., BELARDO, G., ROSSI, A. & SANTORO, M. G. 2001. Activation of I kappa b kinase by herpes simplex virus type 1. A novel target for anti-herpetic therapy. *J Biol Chem* **276**: 28759-28766.DOI: https://doi.org/10.1074/jbc.M103408200, PMID: 11387335

AMICI, C., BELARDO, G., ROZERA, C., BERNASCONI, D. & SANTORO, M. G. 2004. Inhibition of herpesvirus-induced HIV-1 replication by cyclopentenone prostaglandins: role of IkappaB kinase (IKK). *Aids* **18**: 1271-1280.DOI: https://doi.org/10.1097/00002030-200406180-00005, PMID: 15362659

ARCHIN, N. M., KIRCHHERR, J. L., SUNG, J. A., CLUTTON, G., SHOLTIS, K., XU, Y., ALLARD, B., STUELKE, E., KASHUBA, A. D., KURUC, J. D., ERON, J., GAY, C. L., GOONETILLEKE, N. & MARGOLIS, D. M. 2017. Interval dosing with the HDAC inhibitor vorinostat effectively reverses HIV latency. *J Clin Invest* **127**: 3126-3135.DOI: https://doi.org/10.1172/jci92684, PMID: 28714868

ARCHIN, N. M., SUNG, J. M., GARRIDO, C., SORIANO-SARABIA, N. & MARGOLIS, D. M. 2014. Eradicating HIV-1 infection: seeking to clear a persistent pathogen. *Nat Rev Microbiol* **12**: 750-764.DOI: https://doi.org/10.1038/nrmicro3352, PMID: 25402363

BISGROVE, D. A., MAHMOUDI, T., HENKLEIN, P. & VERDIN, E. 2007. Conserved P-TEFb-interacting domain of BRD4 inhibits HIV transcription. *Proc Natl Acad Sci U S A* **104**: 13690-13695.DOI: https://doi.org/10.1073/pnas.0705053104, PMID: 17690245

BONNER, J. J., CHEN, D., STOREY, K., TUSHAN, M. & LEA, K. 2000. Structural analysis of yeast HSF by site-specific crosslinking. *J Mol Biol* **302**: 581-592.DOI: https://doi.org/10.1006/jmbi.2000.4096, PMID: 10986120

CALISTRI, A., PAROLIN, C. & PALù, G. 2003. Herpes simplex virus type 1 can either suppress or enhance human immunodeficiency virus type 1 replication in CD4-positive T lymphocytes. *J Med Virol* **70**: 163-170.DOI: https://doi.org/10.1002/jmv.10350, PMID: 12629659

CHAPMAN, C. J., HARRIS, J. D., COLLINS, M. K. L. & LATCHMAN, D. S. 1991. A recombinant HIV provirus is synergistically activated by the HIV Tat protein and the HSV IE1 protein but not by the HSV IE3 protein. *AIDS* **5**,

CHURCHILL, M. J., DEEKS, S. G., MARGOLIS, D. M., SILICIANO, R. F. & SWANSTROM, R. 2016. HIV reservoirs: what, where and how to target them. *Nat Rev Microbiol* **14**: 55-60.DOI: https://doi.org/10.1038/nrmicro.2015.5, PMID: 26616417

COLLINS, D. R., GAIHA, G. D. & WALKER, B. D. 2020. CD8(+) T cells in HIV control, cure and prevention. *Nat Rev Immunol* **20**: 471-482.DOI: https://doi.org/10.1038/s41577-020-0274-9, PMID: 32051540

DASH, P. K., CHEN, C., KAMINSKI, R., SU, H., MANCUSO, P., SILLMAN, B., ZHANG, C., LIAO, S., SRAVANAM, S., LIU, H., WAIGHT, E., GUO, L., MATHEWS, S., SARIYER, R., MOSLEY, R. L., POLUEKTOVA, L. Y., CAOCCI, M., AMINI, S., GORANTLA, S., BURDO, T. H., EDAGWA, B., GENDELMAN, H. E. & KHALILI, K. 2023. CRISPR editing of CCR5 and HIV-1 facilitates viral elimination in antiretroviral drug-suppressed virus-infected humanized mice. *Proc Natl Acad Sci U S A* **120**: e2217887120.DOI: https://doi.org/10.1073/pnas.2217887120, PMID: 37126704

DASHTI, A., SUKKESTAD, S., HORNER, A. M., NEJA, M., SIDDIQI, Z., WALLER, C., GOLDY, J., MONROE, D., LIN, A., SCHOOF, N., SINGH, V., MAVIGNER, M., LIFSON, J. D., DELEAGE, C., TUYISHIME, M., FALCINELLI, S. D., KING, H. A. D., KE, R., MASON, R. D., ARCHIN, N. M., DUNHAM, R. M., SAFRIT, J. T., JEAN, S., PERELSON, A. S., MARGOLIS, D. M., FERRARI, G., ROEDERER, M., SILVESTRI, G. &

573 CHAHROUDI, A. 2023. AZD5582 plus SIV-specific antibodies reduce lymph node viral reservoirs in
574 antiretroviral therapy-suppressed macaques. *Nat Med*.DOI: https://doi.org/10.1038/s41591-023-
575 02570-7, PMID: 37783968
576 DEEKS, S. G. 2012. HIV: Shock and kill. *Nature* **487**: 439-440.DOI:
577 https://doi.org/10.1038/487439a, PMID: 22836995
578 FARASSATI, F., YANG, A. D. & LEE, P. W. 2001. Oncogenes in Ras signalling pathway dictate host-cell
579 permissiveness to herpes simplex virus 1. *Nat Cell Biol* **3**: 745-750.DOI:
580 https://doi.org/10.1038/35087061, PMID: 11483960
581 FERRE, A. L., HUNT, P. W., CRITCHFIELD, J. W., YOUNG, D. H., MORRIS, M. M., GARCIA, J. C.,
582 POLLARD, R. B., YEE, H. F., JR., MARTIN, J. N., DEEKS, S. G. & SHACKLETT, B. L. 2009. Mucosal
583 immune responses to HIV-1 in elite controllers: a potential correlate of immune control. *Blood* **113**:
584 3978-3989.DOI: https://doi.org/10.1182/blood-2008-10-182709, PMID: 19109229
585 GOLDEN, M. P., KIM, S., HAMMER, S. M., LADD, E. A., SCHAFFER, P. A., DELUCA, N. & ALBRECHT,
586 M. A. 1992. Activation of human immunodeficiency virus by herpes simplex virus. *J Infect Dis* **166**:
587 494-499.DOI: https://doi.org/10.1093/infdis/166.3.494, PMID: 1354237
588 HE, B., GROSS, M. & ROIZMAN, B. 1997. The gamma(1)34.5 protein of herpes simplex virus 1
589 complexes with protein phosphatase 1alpha to dephosphorylate the alpha subunit of the
590 eukaryotic translation initiation factor 2 and preclude the shutoff of protein synthesis by double-
591 stranded RNA-activated protein kinase. *Proc Natl Acad Sci U S A* **94**: 843-848.DOI:
592 https://doi.org/10.1073/pnas.94.3.843, PMID: 9023344
593 HE, B., GROSS, M. & ROIZMAN, B. 1998. The gamma134.5 protein of herpes simplex virus 1 has
594 the structural and functional attributes of a protein phosphatase 1 regulatory subunit and is
595 present in a high molecular weight complex with the enzyme in infected cells. *J Biol Chem* **273**:
596 20737-20743.DOI: https://doi.org/10.1074/jbc.273.33.20737, PMID: 9694816
597 HE, Y., WU, C., LIU, Z., ZHANG, Y., FENG, F., LIN, Z., WANG, C., YANG, Q., WEN, Z., LIU, Y., ZHANG, F.,
598 LIN, Y., ZHANG, H., QU, L., LI, L., CAI, W., SUN, C., CHEN, L. & LI, P. 2023. Arsenic trioxide-induced
599 apoptosis contributes to suppression of viral reservoir in SIV-infected rhesus macaques. *Microbiol*
600 *Spectr*: e0052523.DOI: https://doi.org/10.1128/spectrum.00525-23, PMID: 37695104
601 HENG, M. C., HENG, S. Y. & ALLEN, S. G. 1994. Co-infection and synergy of human
602 immunodeficiency virus-1 and herpes simplex virus-1. *Lancet* **343**: 255-258.DOI:
603 https://doi.org/10.1016/s0140-6736(94)91110-x, PMID: 7905094
604 HERZIG, E., KIM, K. C., PACKARD, T. A., VARDI, N., SCHWARZER, R., GRAMATICA, A., DEEKS, S. G.,
605 WILLIAMS, S. R., LANDGRAF, K., KILLEEN, N., MARTIN, D. W., WEINBERGER, L. S. & GREENE, W. C.
606 2019. Attacking Latent HIV with convertibleCAR-T Cells, a Highly Adaptable Killing Platform. *Cell*
607 **179**: 880-894.e810.DOI: https://doi.org/10.1016/j.cell.2019.10.002, PMID: 31668804
608 JIN, H., YAN, Z., MA, Y., CAO, Y. & HE, B. 2011. A herpesvirus virulence factor inhibits dendritic cell
609 maturation through protein phosphatase 1 and Ikappa B kinase. *J Virol* **85**: 3397-3407.DOI:
610 https://doi.org/10.1128/jvi.02373-10, PMID: 21248029
611 KAUR, A., SANFORD, H. B., GARRY, D., LANG, S., KLUMPP, S. A., WATANABE, D., BRONSON, R. T.,
612 LIFSON, J. D., ROSATI, M., PAVLAKIS, G. N., FELBER, B. K., KNIPE, D. M. & DESROSIERS, R. C. 2007.
613 Ability of herpes simplex virus vectors to boost immune responses to DNA vectors and to protect
614 against challenge by simian immunodeficiency virus. *Virology* **357**: 199-214.DOI:
615 https://doi.org/10.1016/j.virol.2006.08.007, PMID: 16962628
616 KIM, Y., ANDERSON, J. L. & LEWIN, S. R. 2018. Getting the "Kill" into "Shock and Kill": Strategies to
617 Eliminate Latent HIV. *Cell Host Microbe* **23**: 14-26.DOI:
618 https://doi.org/10.1016/j.chom.2017.12.004, PMID: 29324227
619 LEHRMAN, G., HOGUE, I. B., PALMER, S., JENNINGS, C., SPINA, C. A., WIEGAND, A., LANDAY, A. L.,

620 COOMBS, R. W., RICHMAN, D. D., MELLORS, J. W., COFFIN, J. M., BOSCH, R. J. & MARGOLIS, D. M.
621 2005. Depletion of latent HIV-1 infection in vivo: a proof-of-concept study. *Lancet* **366**: 549-
622 555.DOI: https://doi.org/10.1016/s0140-6736(05)67098-5, PMID: 16099290
623 LEITMAN, E. M., THOBAKGALE, C. F., ADLAND, E., ANSARI, M. A., RAGHWANI, J., PRENDERGAST, A.
624 J., TUDOR-WILLIAMS, G., KIEPIELA, P., HEMELAAR, J., BRENER, J., TSAI, M. H., MORI, M., RIDDELL,
625 L., LUZZI, G., JOOSTE, P., NDUNG'U, T., WALKER, B. D., PYBUS, O. G., KELLAM, P., NARANBHAI, V.,
626 MATTHEWS, P. C., GALL, A. & GOULDER, P. J. R. 2017. Role of HIV-specific CD8(+) T cells in pediatric
627 HIV cure strategies after widespread early viral escape. *J Exp Med* **214**: 3239-3261.DOI:
628 https://doi.org/10.1084/jem.20162123, PMID: 28983013
629 LI, Y., ZHANG, C., CHEN, X., YU, J., WANG, Y., YANG, Y., DU, M., JIN, H., MA, Y., HE, B. & CAO, Y. 2011.
630 ICP34.5 protein of herpes simplex virus facilitates the initiation of protein translation by bridging
631 eukaryotic initiation factor 2alpha (eIF2alpha) and protein phosphatase 1. *J Biol Chem* **286**: 24785-
632 24792.DOI: https://doi.org/10.1074/jbc.M111.232439, PMID: 21622569
633 LI, Z., GUO, J., WU, Y. & ZHOU, Q. 2013. The BET bromodomain inhibitor JQ1 activates HIV latency
634 through antagonizing Brd4 inhibition of Tat-transactivation. *Nucleic Acids Res* **41**: 277-287.DOI:
635 https://doi.org/10.1093/nar/gks976, PMID: 23087374
636 LIN, J., ZHANG, X., LU, W., XU, X., PAN, X., LIANG, T., DUAN, S., CHEN, Y., LI, L. & LIU, S. 2018. PR-
637 957, a selective immunoproteasome inhibitor, reactivates latent HIV-1 through p-TEFb activation
638 mediated by HSF-1. *Biochem Pharmacol* **156**: 511-523.DOI:
639 https://doi.org/10.1016/j.bcp.2018.08.042, PMID: 30170098
640 LOOKER, K. J., ELMES, J. A. R., GOTTLIEB, S. L., SCHIFFER, J. T., VICKERMAN, P., TURNER, K. M. E. &
641 BOILY, M. C. 2017. Effect of HSV-2 infection on subsequent HIV acquisition: an updated systematic
642 review and meta-analysis. *Lancet Infect Dis* **17**: 1303-1316.DOI: https://doi.org/10.1016/s1473-
643 3099(17)30405-x, PMID: 28843576
644 MALDINI, C. R., CLAIBORNE, D. T., OKAWA, K., CHEN, T., DOPKIN, D. L., SHAN, X., POWER, K. A.,
645 TRIFONOVA, R. T., KRUPP, K., PHELPS, M., VRBANAC, V. D., TANNO, S., BATESON, T., LESLIE, G. J.,
646 HOXIE, J. A., BOUTWELL, C. L., RILEY, J. L. & ALLEN, T. M. 2020. Dual CD4-based CAR T cells with
647 distinct costimulatory domains mitigate HIV pathogenesis in vivo. *Nat Med* **26**: 1776-1787.DOI:
648 https://doi.org/10.1038/s41591-020-1039-5, PMID: 32868878
649 MANIVANH, R., MEHRBACH, J., KNIPE, D. M. & LEIB, D. A. 2017. Role of Herpes Simplex Virus 1
650 γ34.5 in the Regulation of IRF3 Signaling. *J Virol* **91**.DOI: https://doi.org/10.1128/jvi.01156-17,
651 PMID: 28904192
652 MOSCA, J. D., BEDNARIK, D. P., RAJ, N. B., ROSEN, C. A., SODROSKI, J. G., HASELTINE, W. A.,
653 HAYWARD, G. S. & PITHA, P. M. 1987a. Activation of human immunodeficiency virus by herpesvirus
654 infection: identification of a region within the long terminal repeat that responds to a trans-acting
655 factor encoded by herpes simplex virus 1. *Proc Natl Acad Sci U S A* **84**: 7408-7412.DOI:
656 https://doi.org/10.1073/pnas.84.21.7408, PMID: 2823260
657 MOSCA, J. D., BEDNARIK, D. P., RAJ, N. B., ROSEN, C. A., SODROSKI, J. G., HASELTINE, W. A. & PITHA,
658 P. M. 1987b. Herpes simplex virus type-1 can reactivate transcription of latent human
659 immunodeficiency virus. *Nature* **325**: 67-70.DOI: https://doi.org/10.1038/325067a0, PMID:
660 3025748
661 MURPHY, C. G., LUCAS, W. T., MEANS, R. E., CZAJAK, S., HALE, C. L., LIFSON, J. D., KAUR, A.,
662 JOHNSON, R. P., KNIPE, D. M. & DESROSIERS, R. C. 2000. Vaccine protection against simian
663 immunodeficiency virus by recombinant strains of herpes simplex virus. *J Virol* **74**: 7745-7754.DOI:
664 https://doi.org/10.1128/jvi.74.17.7745-7754.2000, PMID: 10933680
665 O'CONNELL, K. A., BAILEY, J. R. & BLANKSON, J. N. 2009. Elucidating the elite: mechanisms of
666 control in HIV-1 infection. *Trends Pharmacol Sci* **30**: 631-637.DOI:

667 https://doi.org/10.1016/j.tips.2009.09.005, PMID: 19837464
668 ORR, M. T., EDELMANN, K. H., VIEIRA, J., COREY, L., RAULET, D. H. & WILSON, C. B. 2005. Inhibition
669 of MHC class I is a virulence factor in herpes simplex virus infection of mice. *PLoS Pathog* **1**: e7.DOI:
670 https://doi.org/10.1371/journal.ppat.0010007, PMID: 16201019
671 ORVEDAHL, A., ALEXANDER, D., TALLóCZY, Z., SUN, Q., WEI, Y., ZHANG, W., BURNS, D., LEIB, D. A.
672 & LEVINE, B. 2007. HSV-1 ICP34.5 confers neurovirulence by targeting the Beclin 1 autophagy
673 protein. *Cell Host Microbe* **1**: 23-35.DOI: https://doi.org/10.1016/j.chom.2006.12.001, PMID:
674 18005679
675 OWEN, R. E., HEITMAN, J. W., HIRSCHKORN, D. F., LANTERI, M. C., BISWAS, H. H., MARTIN, J. N.,
676 KRONE, M. R., DEEKS, S. G. & NORRIS, P. J. 2010. HIV+ elite controllers have low HIV-specific T-cell
677 activation yet maintain strong, polyfunctional T-cell responses. *Aids* **24**: 1095-1105.DOI:
678 https://doi.org/10.1097/QAD.0b013e3283377a1e, PMID: 20400885
679 PAN, E., FENG, F., LI, P., YANG, Q., MA, X., WU, C., ZHAO, J., YAN, H., CHEN, R., CHEN, L. & SUN, C.
680 2018. Immune Protection of SIV Challenge by PD-1 Blockade During Vaccination in Rhesus
681 Monkeys. *Front Immunol* **9**: 2415.DOI: https://doi.org/10.3389/fimmu.2018.02415, PMID:
682 30405615
683 PAN, X. Y., ZHAO, W., WANG, C. Y., LIN, J., ZENG, X. Y., REN, R. X., WANG, K., XUN, T. R., SHAI, Y. &
684 LIU, S. W. 2016a. Heat Shock Protein 90 Facilitates Latent HIV Reactivation through Maintaining
685 the Function of Positive Transcriptional Elongation Factor b (p-TEFb) under Proteasome Inhibition.
686 *J Biol Chem* **291**: 26177-26187.DOI: https://doi.org/10.1074/jbc.M116.743906, PMID: 27799305
687 PAN, X. Y., ZHAO, W., ZENG, X. Y., LIN, J., LI, M. M., SHEN, X. T. & LIU, S. W. 2016b. Heat Shock Factor
688 1 Mediates Latent HIV Reactivation. *Sci Rep* **6**: 26294.DOI: https://doi.org/10.1038/srep26294,
689 PMID: 27189267
690 PANDREA, I., GAUFIN, T., GAUTAM, R., KRISTOFF, J., MANDELL, D., MONTEFIORI, D., KEELE, B. F.,
691 RIBEIRO, R. M., VEAZEY, R. S. & APETREI, C. 2011. Functional cure of SIVagm infection in rhesus
692 macaques results in complete recovery of CD4+ T cells and is reverted by CD8+ cell depletion. *PLoS*
693 *Pathog* **7**: e1002170.DOI: https://doi.org/10.1371/journal.ppat.1002170, PMID: 21829366
694 PARKER, S. D., ROTTINGHAUS, S. T., ZAJAC, A. J., YUE, L., HUNTER, E., WHITLEY, R. J. & PARKER, J.
695 N. 2007. HIV-1(89.6) Gag expressed from a replication competent HSV-1 vector elicits persistent
696 cellular immune responses in mice. *Vaccine* **25**: 6764-6773.DOI:
697 https://doi.org/10.1016/j.vaccine.2007.06.064, PMID: 17706843
698 PENG, W., HONG, Z., CHEN, X., GAO, H., DAI, Z., ZHAO, J., LIU, W., LI, D. & DENG, K. 2020.
699 Thiostrepton Reactivates Latent HIV-1 through the p-TEFb and NF-κB Pathways Mediated by Heat
700 Shock Response. *Antimicrob Agents Chemother* **64**.DOI: https://doi.org/10.1128/aac.02328-19,
701 PMID: 32094131
702 PERDOMO-CELIS, F., PASSAES, C., MONCEAUX, V., VOLANT, S., BOUFASSA, F., DE TRUCHIS, P.,
703 MARCOU, M., BOURDIC, K., WEISS, L., JUNG, C., BOURGEOIS, C., GOUJARD, C., MEYER, L., MüLLER-
704 TRUTWIN, M., LAMBOTTE, O. & SáEZ-CIRIóN, A. 2022. Reprogramming dysfunctional CD8+ T cells
705 to promote properties associated with natural HIV control. *J Clin Invest* **132**.DOI:
706 https://doi.org/10.1172/jci157549, PMID: 35380989
707 PIERCE, C. A., LOH, L. N., STEACH, H. R., CHESHENKO, N., PRESTON-HURLBURT, P., ZHANG, F.,
708 STRANSKY, S., KRAVETS, L., SIDOLI, S., PHILBRICK, W., NASSAR, M., KRISHNASWAMY, S., HEROLD,
709 K. C. & HEROLD, B. C. 2023. HSV-2 triggers upregulation of MALAT1 in CD4+ T cells and promotes
710 HIV latency reversal. *J Clin Invest* **133**.DOI: https://doi.org/10.1172/jci164317, PMID: 37079384
711 PIERSON, T., MCARTHUR, J. & SILICIANO, R. F. 2000. Reservoirs for HIV-1: mechanisms for viral
712 persistence in the presence of antiviral immune responses and antiretroviral therapy. *Annu Rev*
713 *Immunol* **18**: 665-708.DOI: https://doi.org/10.1146/annurev.immunol.18.1.665, PMID: 10837072

714 POH, A. 2016. First Oncolytic Viral Therapy for Melanoma. *Cancer Discov* **6**: 6.DOI:
715 https://doi.org/10.1158/2159-8290.Cd-nb2015-158, PMID: 26552414
716 RAWAT, P. & MITRA, D. 2011. Cellular heat shock factor 1 positively regulates human
717 immunodeficiency virus-1 gene expression and replication by two distinct pathways. *Nucleic Acids*
718 *Res* **39**: 5879-5892.DOI: https://doi.org/10.1093/nar/gkr198, PMID: 21459854
719 SUN, C., ZHANG, L., ZHANG, M., LIU, Y., ZHONG, M., MA, X. & CHEN, L. 2010. Induction of balance
720 and breadth in the immune response is beneficial for the control of SIVmac239 replication in
721 rhesus monkeys. *J Infect* **60**: 371-381.DOI: https://doi.org/10.1016/j.jinf.2010.03.005, PMID:
722 20227437
723 TIMMONS, A., FRAY, E., KUMAR, M., WU, F., DAI, W., BULLEN, C. K., KIM, P., HETZEL, C., YANG, C.,
724 BEG, S., LAI, J., POMERANTZ, J. L., YUKL, S. A., SILICIANO, J. D. & SILICIANO, R. F. 2020. HSF1
725 inhibition attenuates HIV-1 latency reversal mediated by several candidate LRAs In Vitro and Ex
726 Vivo. *Proc Natl Acad Sci U S A* **117**: 15763-15771.DOI: https://doi.org/10.1073/pnas.1916290117,
727 PMID: 32571938
728 TRAUTMANN, L., JANBAZIAN, L., CHOMONT, N., SAID, E. A., GIMMIG, S., BESSETTE, B., BOULASSEL,
729 M. R., DELWART, E., SEPULVEDA, H., BALDERAS, R. S., ROUTY, J. P., HADDAD, E. K. & SEKALY, R. P.
730 2006. Upregulation of PD-1 expression on HIV-specific CD8+ T cells leads to reversible immune
731 dysfunction. *Nat Med* **12**: 1198-1202.DOI: https://doi.org/10.1038/nm1482, PMID: 16917489
732 VLACH, J. & PITHA, P. M. 1992. Herpes simplex virus type 1-mediated induction of human
733 immunodeficiency virus type 1 provirus correlates with binding of nuclear proteins to the NF-
734 kappa B enhancer and leader sequence. *J Virol* **66**: 3616-3623.DOI:
735 https://doi.org/10.1128/jvi.66.6.3616-3623.1992, PMID: 1316471
736 VLACH, J. & PITHA, P. M. 1993. Differential contribution of herpes simplex virus type 1 gene
737 products and cellular factors to the activation of human immunodeficiency virus type 1 provirus.
738 *J Virol* **67**: 4427-4431.DOI: https://doi.org/10.1128/jvi.67.7.4427-4431.1993, PMID: 8389940
739 WALKER-SPERLING, V. E. K., MERCADO, N. B., CHANDRASHEKAR, A., BORDUCCHI, E. N., LIU, J.,
740 NKOLOLA, J. P., LEWIS, M., MURRY, J. P., YANG, Y., GELEZIUNAS, R., ROBB, M. L., MICHAEL, N. L.,
741 PAU, M. G., WEGMANN, F., SCHUITEMAKER, H., FRAY, E. J., KUMAR, M. R., SILICIANO, J. D.,
742 SILICIANO, R. F. & BAROUCH, D. H. 2022. Therapeutic efficacy of combined active and passive
743 immunization in ART-suppressed, SHIV-infected rhesus macaques. *Nat Commun* **13**: 3463.DOI:
744 https://doi.org/10.1038/s41467-022-31196-5, PMID: 35710819
745 WU, C., HE, Y., ZHAO, J., LUO, K., WEN, Z., ZHANG, Y., LI, M., CUI, Y., LIU, Z., WANG, C., HAN, Z., LI,
746 G., FENG, F., LI, P., CHEN, L. & SUN, C. 2022. Exacerbated AIDS Progression by PD-1 Blockade during
747 Therapeutic Vaccination in Chronically Simian Immunodeficiency Virus-Infected Rhesus Macaques
748 after Interruption of Antiretroviral Therapy. *J Virol* **96**: e0178521.DOI:
749 https://doi.org/10.1128/JVI.01785-21, PMID: 34818070
750 WU, C., ZHAO, J., LI, R., FENG, F., HE, Y., LI, Y., HUANG, R., LI, G., YANG, H., CHENG, G., CHEN, L.,
751 MA, F., LI, P. & SUN, C. 2021. Modulation of Antiviral Immunity and Therapeutic Efficacy by 25-
752 Hydroxycholesterol in Chronically SIV-Infected, ART-Treated Rhesus Macaques. *Virol Sin* **36**: 1197-
753 1209.DOI: https://doi.org/10.1007/s12250-021-00407-6, PMID: 34057681
754 XIAO, L., WANG, D., SUN, C., LI, P., JIN, Y., FENG, L. & CHEN, L. 2014. Enhancement of SIV-specific
755 cell mediated immune responses by co-administration of soluble PD-1 and Tim-3 as molecular
756 adjuvants in mice. *Hum Vaccin Immunother* **10**: 724-733.DOI: https://doi.org/10.4161/hv.27340,
757 PMID: 24326266
758 XU, X., LIN, Y., ZENG, X., YANG, C., DUAN, S., DING, L., LU, W., LIN, J., PAN, X., MA, X. & LIU, S. 2022.
759 PARP1 Might Substitute HSF1 to Reactivate Latent HIV-1 by Binding to Heat Shock Element. *Cells*
760 **11**.DOI: https://doi.org/10.3390/cells11152331, PMID: 35954175

761 YANG, Q., FENG, F., LI, P., PAN, E., WU, C., HE, Y., ZHANG, F., ZHAO, J., LI, R., FENG, L., HU, F., LI, L.,
762 ZOU, H., CAI, W., LEHNER, T., SUN, C. & CHEN, L. 2019. Arsenic Trioxide Impacts Viral Latency and
763 Delays Viral Rebound after Termination of ART in Chronically SIV-Infected Macaques. *Adv Sci*
764 *(Weinh)* **6**: 1900319.DOI: https://doi.org/10.1002/advs.201900319, PMID: 31380187
765 YEH, Y. J. & HO, Y. C. 2021. Shock-and-kill versus block-and-lock: Targeting the fluctuating and
766 heterogeneous HIV-1 gene expression. *Proc Natl Acad Sci U S A* **118**.DOI:
767 https://doi.org/10.1073/pnas.2103692118, PMID: 33758027
768 ZENG, X., PAN, X., XU, X., LIN, J., QUE, F., TIAN, Y., LI, L. & LIU, S. 2017. Resveratrol Reactivates
769 Latent HIV through Increasing Histone Acetylation and Activating Heat Shock Factor 1. *J Agric Food*
770 *Chem* **65**: 4384-4394.DOI: https://doi.org/10.1021/acs.jafc.7b00418, PMID: 28471170
771 ZHAO, J., CHEN, J., WANG, C., LIU, Y., LI, M., LI, Y., LI, R., HAN, Z., WANG, J., CHEN, L., SHU, Y., CHENG,
772 G. & SUN, C. 2022. Kynurenine-3-monooxygenase (KMO) broadly inhibits viral infections via
773 triggering NMDAR/Ca2+ influx and CaMKII/ IRF3-mediated IFN-beta production. *PLoS Pathog* **18**:
774 e1010366.DOI: https://doi.org/10.1371/journal.ppat.1010366, PMID: 35235615
775 ZHOU, J., CHEUNG, A. K., TAN, Z., WANG, H., YU, W., DU, Y., KANG, Y., LU, X., LIU, L., YUEN, K. Y. &
776 CHEN, Z. 2013. PD1-based DNA vaccine amplifies HIV-1 GAG-specific CD8+ T cells in mice. *J Clin*
777 *Invest* **123**: 2629-2642.DOI: https://doi.org/10.1172/jci64704, PMID: 23635778
778

779

Figure Legends

Figure 1. The modified HSV-ΔICP34.5-based constructs reactivated HIV latency more efficiently than wild-type HSV counterparts. (**A**) J-Lat 10.6 cells (1×10^6) were infected with varying MOIs of wild-type HSV-1 17 strain for 30 h. The increasing expression level of GFP^+ cells with increasing MOI of HSV-1 was displayed with the pseudocolor plot (left) and the corresponding bar chart (right). (**B**) The mRNA levels of HIV-1 LTR, Tat, Gag, Vpr, and Vif in J-Lat 10.6 cells following infection with the wild-type HSV-1 17 strain were shown with the histogram. (**C**) J-Lat 10.6 cells (1×10^6) were infected with HSV-wt or HSV-ΔICP34.5 at an MOI of 0.1 for 30 h, and then the mRNA levels of HIV-1 LTR, Tat, Gag, Vpr, Vif, and (**D**) HSV-1 UL27 were shown with the histogram. (**E**) ACH-2 cells (1×10^6) were infected with HSV-wt or HSV-ΔICP34.5 at an MOI of 0.1 for 30 h, and then the p24 protein level was detected using an HIV-1 p24 ELISA kit. (**F**) ACH-2 cells (1×10^6) were infected with HSV-wt or HSV-ΔICP34.5 at an MOI of 0.1 for 30 h, and then the mRNA levels of HIV-1 LTR, Tat, Gag, Vpr and Vif were shown with the histogram. (**G**) J-Lat 10.6 and J-Lat 10.6-ICP34.5 cells were infected with HSV-wt or HSV-ΔICP34.5, and then the mRNA levels of HIV-1 Tat were shown with the histogram (left). The blotting showed that the J-Lat 10.6 cells stably expressing HSV ICP34.5 (J-Lat 10.6-ICP34.5) can appropriately express ICP34.5 protein using Flag-tag antibodies (right). (**H**) J-Lat 10.6 and J-Lat 10.6-ICP34.5 cells were respectively stimulated with PMA (10 ng/mL) and TNF-α (10 ng/mL), and the expression level of GFP^+ cells was displayed with the corresponding bar chart. Data shown are mean ± SD. **P<0.01, ***P<0.001, ****P<0.0001. ns: no significance.

Figure 2. The modified HSV-based constructs effectively reactivated HIV latency by modulating the NF-κB pathway and HSF1 pathway. (**A**) J-Lat 10.6 cells were infected with HSV-wt and HSV-ΔICP34.5 at an MOI of 0.1. The cytoplasmic and nuclear proteins were separated to detect the expression level of p65, p-IKKα/β and IkBα. GAPDH and Lamin B1 served as loading controls for cytoplasmic and nuclear proteins, respectively. (**B**) 293T cells were transfected with Flag-ICP34.5, IKKα (left), or IKKβ (right), and the cell lysates and IP complexes were analyzed through Co-IP assays. (**C**) 293T cells were transfected with Flag-ICP34.5 or empty vector (Vec) for 24h, and then treated with LPS (1μg/mL) for 8h. The cytoplasmic and nuclear proteins were analyzed by Western blotting (WB) assay. (**D-E**) J-Lat 10.6 cells were infected with HSV-ΔICP34.5 and then treated with different concentrations of KRIBB11. The relative fold change in LTR and Tat mRNA was analyzed by qPCR. (**F**) J-Lat 10.6 cells were infected with HSV-wt or HSV-ΔICP34.5 at MOI of 0.1 for 36h. ChIP-qPCR was conducted to evaluate the ability of HSF1 to bind to the LTR. IgG and Histone antibody (His) were used as negative and positive controls, respectively. (**G**) 293T cells were transfected with Flag-ICP34.5 and Myc-HSF1, and the cell lysates and IP complexes were analyzed through Co-IP assays. (**H**) 293T cells were transfected with 0, 1, 2, 4 μg of Flag-ICP34.5 and analyzed by WB analysis. (**I**) 293T cells were transfected with Flag-ICP34.5 and HA-PP1α, and the cell lysates and IP

complexes were analyzed through Co-IP assays. (**J**) 293T cells were transfected with 0, 0.5, 1, 2 μg of HA-PP1α and analyzed by WB analysis. 293T cells were transfected with Myc-HSF1 with or without Flag-ICP34.5 (**K**), or were transfected with Myc-HSF1 and HA-PP1α (**L**), and then the cell lysates and IP complexes were analyzed through Co-IP assays. Data shown are mean ± SD. ***P*<0.01, ****P*<0.0001. ns: no significance.

Figure 3. Recombinant HSV-1 vector-based SIV vaccines induce specific T cell immune responses in mice. (**A**) The schematic diagram illustrated the process of constructing recombinant HSV through the BAC/galK selection system. Firstly, ICP34.5 gene was replaced with galK gene through homologous recombination. Subsequently, galK was substituted with the target gene expression cassette containing the hCMV promoter and BGH terminator. Finally, the ICP47 gene was deleted. (**B**) The image of one clone of the rescued recombinant HSV with the brightfield (top) and the fluorescence channel (bottom). (**C**) Vero cells were infected with recombinant HSV constructs, and the protein expression of targeted genes was detected by using SIV-infected monkey serum. (**D**) HeLa cells were transfected with Myc-PDL1, followed by infection with HSV-empty, HSV-SIVgag, or HSV-sPD1-SIVgag at an MOI of 0.1 for 24 h. The cell lysates were subjected to Co-IP analysis. (**E**) Schematic schedule of vaccinated mice. Twenty-five mice were randomly allocated to five groups, HSV-empty, HSV-sPD1, HSV-SIVgag, HSV-sPD1-SIVgag, and HSV-SIVenv. At week 0 and week 2, mice were injected with the corresponding vaccines. At week 4, mice were sacrificed and spleen lymphocytes were collected to evaluate immune response. (**F-G**) Column graphs depicted the Gag or Env1, Env2-specific spot-forming cells (SFCs) per 10^6 spleen lymphocytes as measured by IFN-γ ELISpot assay. (**H**) The pseudocolor plot of flow cytometry illustrated the gating strategy. Column graphs depicted the frequencies of IFN-γ, IL-2, and TNF-α production from gag-specific $CD3^+$ T (**I**), $CD4^+$ T (**J**), and $CD8^+$ T cells (**K**). (**L**) The bar chart illustrated the proportion of Tem of $CD4^+$ T and $CD8^+$ T cells under stimulation with the SIV Gag peptide pools. (**M**) The bar chart illustrated the frequencies of Env2-specific IFN-γ^+ $CD4^+$ T cells. These data were expressed as the mean±SD from five mice samples. Three independent experiments for the animal immunization were repeated. **P*<0.05, ***P*<0.01, ****P*<0.001, ****P*<0.0001. ns: no significance.

Figure 4. The modified HSV-based constructs efficiently elicited SIV-specific immune responses in chronically SIV-infected macaques. (**A**) Schematic schedule of the macaque experiment. Nine chronically SIV-infected macaques were assigned into three groups: ART+saline group (n=3), ART+HSV-empty group (n=3), and ART+HSV-sPD1-SIVgag/SIVenv group (n=3). All SIV-infected macaques received ART treatment (FTC/6.7 mg/kg/once daily, PMPA/10 mg/kg/once daily) for 33 days. On day 33 and day 52, macaques were immunized with saline, HSV-empty, and HSV-sPD1-SIVgag/SIVenv respectively. On day 70 after the second vaccination, ART treatment was interrupted in all macaques. Samples were collected at different time points to monitor virological and immunological parameters. (**B**) The representative images for the Gag or Env-

specific spots (2.5×10^5 cells per well) of each macaque pre-vaccination (before, day 33) and post-vaccination (after, day 70) by ELISpot assay. (**C-D**) The difference in SIV-specific IFN-γ-secreting cells (ΔSFCs) between pre-immunization and post-immunization for the assessment of the immune response induced by HSV-vectored SIV vaccines. (**E**) The difference in SIV-specific TNF-α/IFN-γ/IL-2-secreting $CD4^+$ T and $CD8^+$ T subsets between pre-immunization and post-immunization was detected by ICS assay.

Figure 5. The modified HSV-based constructs effectively reactivated SIV latency in vivo in chronically SIV-infected, ART-treated macaques. (**A-D**) The viral load (VL) change in plasma for each animal was monitored during the whole experiment by y real-time PCR. The detection limit is 100 copies per mL plasma. The shadow represented the duration of ART administration. (**E**) The VL change in plasma between pre-ART and the peak value in the rebound stage after ART discontinuation. (**F**) The change of total SIV DNA copies between pre-ART and viral rebound after ART discontinuation. (**G**) The change of the SIV Pol-specific IFN-γ-secreting cells between pre-immunization (day 33) and post-immunization (day 70) was detected by ELISpot assay. (**H**) The change of the $CD4^+$ T/ $CD8^+$ T ratio.

Figure 6. Pattern to illustrate the proof-of-concept strategy based on a bifunctional HSV-vectored therapeutic vaccine for HIV functional cure. In the present study, the modified HSV-ΔICP34.5-based constructs effectively reactivated HIV/SIV latency by modulating the IKKα/β-NF-κB pathway and PP1-HSF1 pathway (Shock) and simultaneously elicited antigen-specific polyfunctional $CD8^+$ T cells to eliminate cells infected with the reactivated virion (Kill). BAC: bacterial artificial chromosome; rHSV: recombinant HSV; TCR: T-cell receptor; PD1: Programmed Cell Death Protein 1; CD40L: CD40 Ligand.

Figure 1

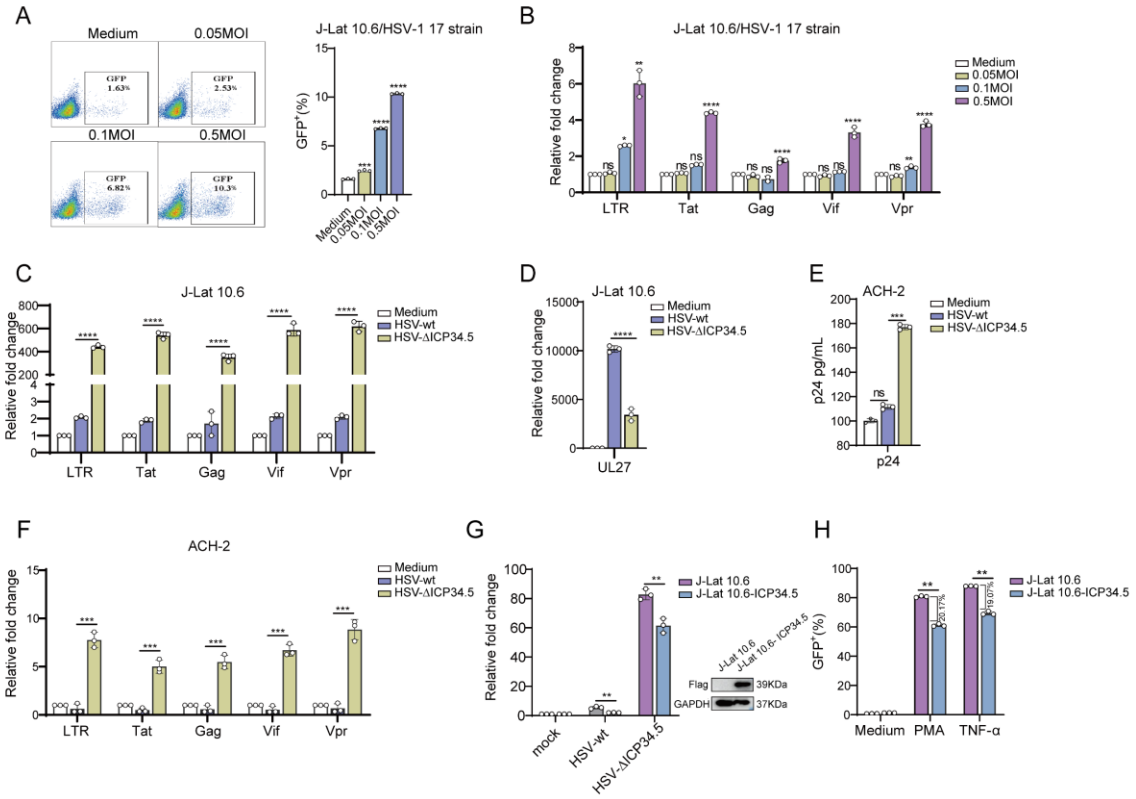
A
Medium
0.05MOI
0.1MOI
0.5MOI
GFP 1.63%
GFP 2.53%
GFP 6.82%
GFP 10.3%
J-Lat 10.6/HSV-1 17 strain
GFP+(%)
Medium
0.05MOI
0.1MOI
0.5MOI
B
J-Lat 10.6/HSV-1 17 strain
Relative fold change
Medium
0.05MOI
0.1MOI
0.5MOI
LTR
Tat
Gag
Vif
Vpr
C
J-Lat 10.6
Relative fold change
Medium
HSV-wt
HSV-ΔICP34.5
LTR
Tat
Gag
Vif
Vpr
D
J-Lat 10.6
Relative fold change
Medium
HSV-wt
HSV-ΔICP34.5
UL27
E
ACH-2
p24 pg/mL
Medium
HSV-wt
HSV-ΔICP34.5
p24
F
ACH-2
Relative fold change
Medium
HSV-wt
HSV-ΔICP34.5
LTR
Tat
Gag
Vif
Vpr
G
Relative fold change
J-Lat 10.6
J-Lat 10.6-ICP34.5
mock
HSV-wt
HSV-ΔICP34.5
J-Lat 10.6
J-Lat 10.6- ICP34.5
Flag
39KDa
GAPDH
37KDa
H
GFP+(%)
J-Lat 10.6
J-Lat 10.6-ICP34.5
Medium
PMA
TNF-α

Figure 2

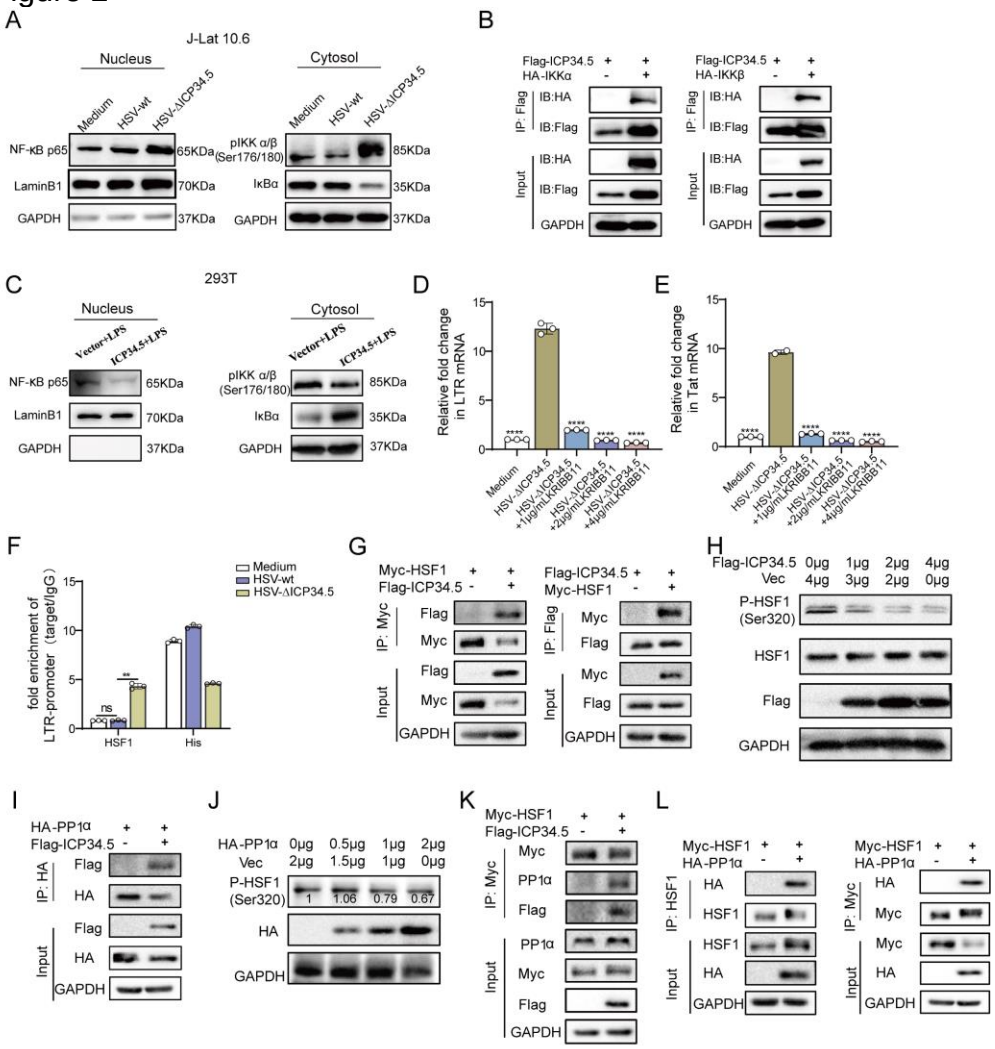
A
J-Lat 10.6
Nucleus
Cytosol
Medium
HSV-wt
HSV-ΔICP34.5
NF-κB p65
LaminB1
GAPDH
pIKK α/β (Ser176/180)
IκBα
65KDa
70KDa
37KDa
85KDa
35KDa
B
Flag-ICP34.5
HA-IKKα
HA-IKKβ
IP: Flag
Input
IB:HA
IB:Flag
C
293T
Vector+LPS
ICP34.5+LPS
D
Relative fold change in LTR mRNA
E
Relative fold change in Tat mRNA
F
fold enrichment of LTR-promoter（target/IgG）
HSF1
His
ns
G
Myc-HSF1
IP: Myc
IP: Flag
H
Flag-ICP34.5
P-HSF1 (Ser320)
I
HA-PP1α
IP: HA
J
K
L
IP: HSF1
IP: Myc

Figure 3

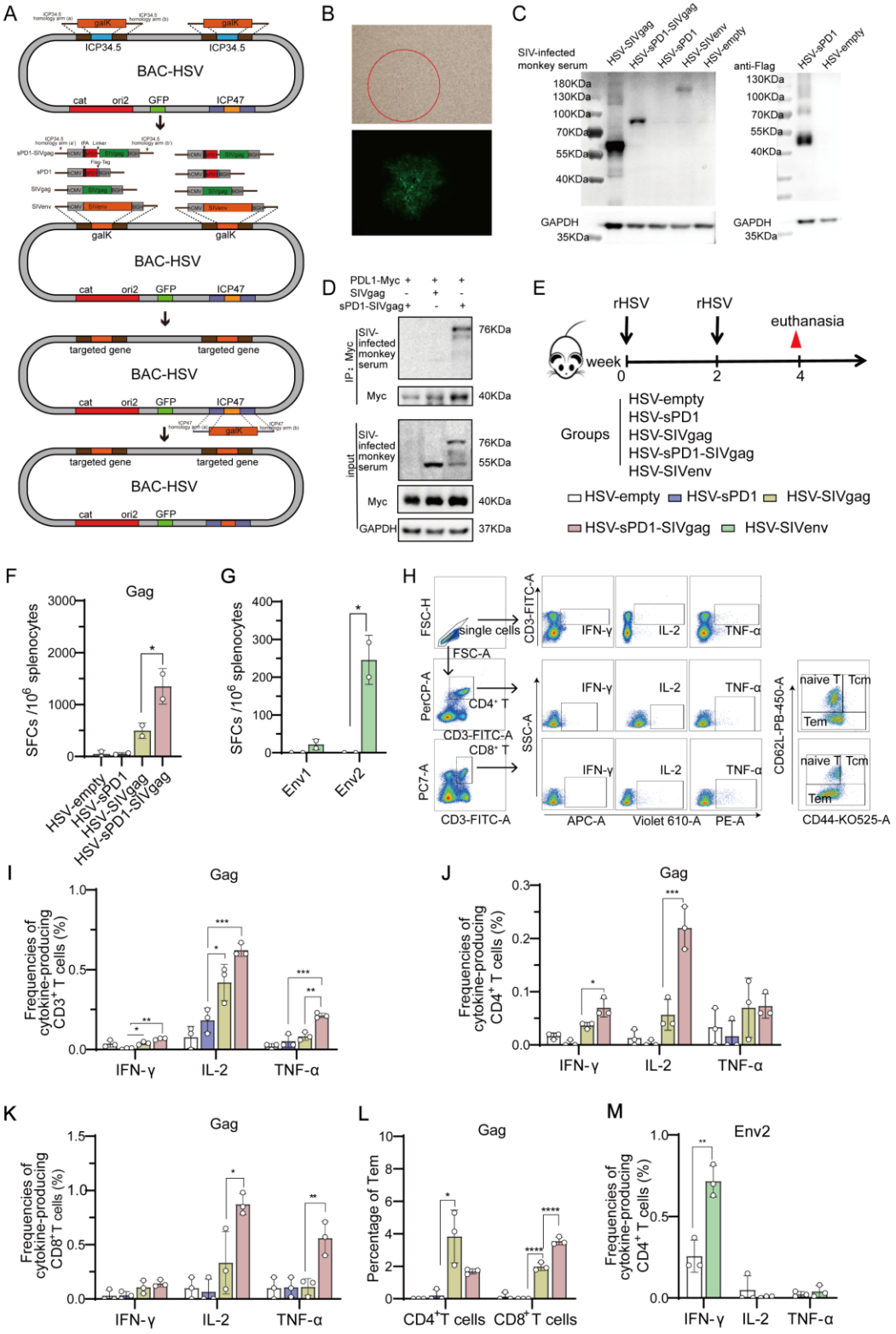
A
ICP34.5
BAC-HSV
cat
ori2
GFP
ICP47
galK
targeted gene
B
C
SIV-infected monkey serum
HSV-SIVgag
HSV-sPD1-SIVgag
HSV-sPD1
HSV-SIVenv
HSV-empty
anti-Flag
180KDa
130KDa
100KDa
70KDa
55KDa
40KDa
GAPDH
35KDa
D
PDL1-Myc
SIVgag
sPD1-SIVgag
IP：Myc
input
Myc
76KDa
40KDa
55KDa
37KDa
E
rHSV
euthanasia
week
0
2
4
Groups
HSV-empty
HSV-sPD1
HSV-SIVgag
HSV-sPD1-SIVgag
HSV-SIVenv
F
Gag
SFCs /10^6 splenocytes
G
Env1
Env2
H
FSC-H
single cells
FSC-A
PerCP-A
CD4+ T
CD3-FITC-A
CD8+ T
PC7-A
SSC-A
IFN-γ
IL-2
TNF-α
APC-A
Violet 610-A
PE-A
CD62L-PB-450-A
naive T
Tcm
Tem
CD44-KO525-A
I
Frequencies of cytokine-producing CD3+ T cells (%)
J
Frequencies of cytokine-producing CD4+ T cells (%)
K
Frequencies of cytokine-producing CD8+ T cells (%)
L
Percentage of Tem
CD4+T cells
CD8+ T cells
M
Env2

Figure 4

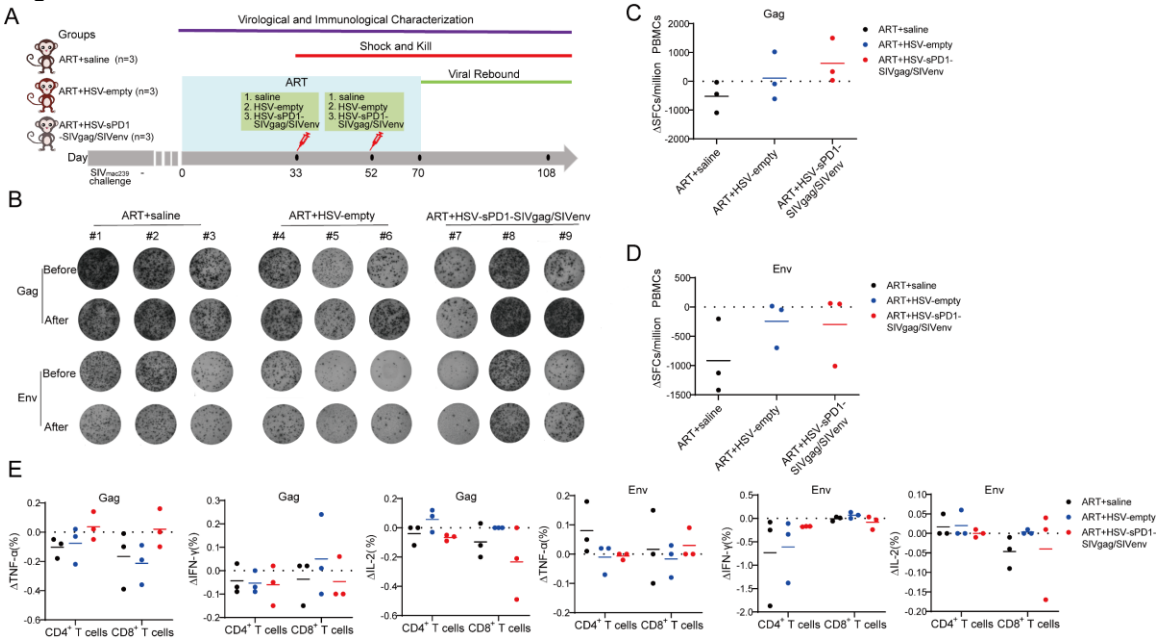
A
Groups
ART+saline (n=3)
ART+HSV-empty (n=3)
ART+HSV-sPD1 -SIVgag/SIVenv (n=3)
Virological and Immunological Characterization
Shock and Kill
Viral Rebound
ART
1. saline
2. HSV-empty
3. HSV-sPD1-SIVgag/SIVenv
Day
0
33
52
70
108
B
ART+saline
ART+HSV-empty
ART+HSV-sPD1-SIVgag/SIVenv
#1
#2
#3
#4
#5
#6
#7
#8
#9
Gag
Env
Before
After
C
Gag
ΔSFCs/million PBMCs
ART+saline
ART+HSV-empty
ART+HSV-sPD1-SIVgag/SIVenv
D
Env
E
Gag
Env
ΔTNF-α(%)
ΔIFN-γ(%)
ΔIL-2(%)
CD4+ T cells
CD8+ T cells

Figure 5

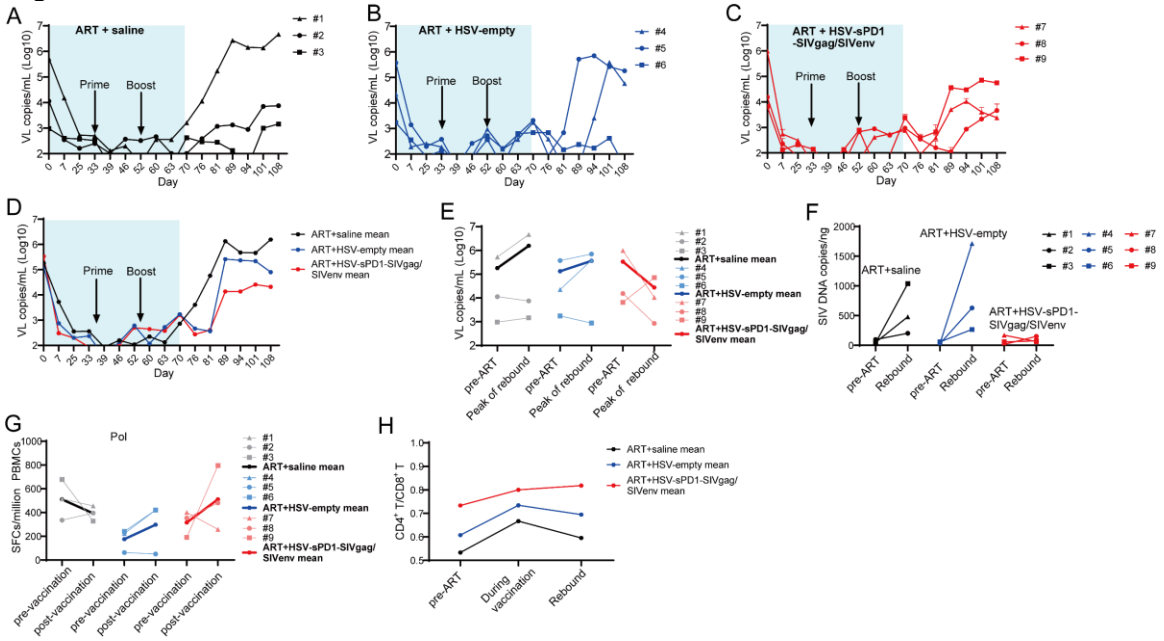
A
ART + saline
Prime
Boost
VL copies/mL (Log10)
Day
#1
#2
#3
B
ART + HSV-empty
#4
#5
#6
C
ART + HSV-sPD1 -SIVgag/SIVenv
#7
#8
#9
D
ART+saline mean
ART+HSV-empty mean
ART+HSV-sPD1-SIVgag/ SIVenv mean
E
pre-ART
Peak of rebound
F
SIV DNA copies/ng
ART+saline
ART+HSV-empty
ART+HSV-sPD1-SIVgag/SIVenv
Rebound
G
Pol
SFCs/million PBMCs
pre-vaccination
post-vaccination
H
CD4+ T/CD8+ T
pre-ART
During vaccination
Rebound

Figure 6

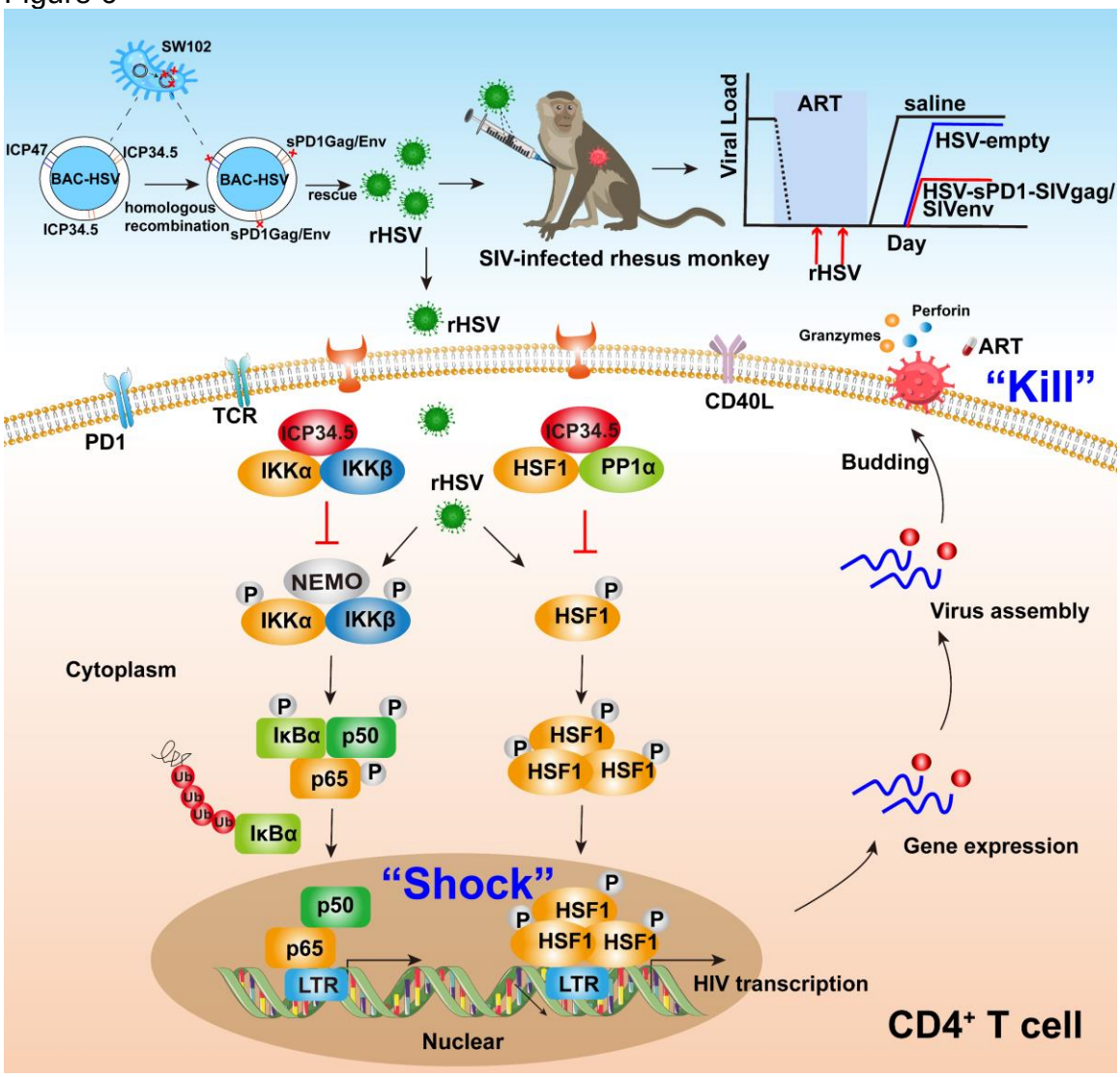
SW102
ICP47
ICP34.5
BAC-HSV
ICP34.5
homologous recombination
BAC-HSV
sPD1Gag/Env
sPD1Gag/Env
rescue
rHSV
SIV-infected rhesus monkey
Viral Load
ART
saline
HSV-empty
HSV-sPD1-SIVgag/SIVenv
Day
rHSV
rHSV
Perforin
Granzymes
ART
"Kill"
CD40L
PD1
TCR
ICP34.5
IKKα
IKKβ
rHSV
ICP34.5
HSF1
PP1α
Budding
NEMO
IKKα
IKKβ
HSF1
Virus assembly
Cytoplasm
IκBα
p50
p65
HSF1
HSF1
HSF1
Ub
IκBα
Gene expression
"Shock"
p50
p65
HSF1
HSF1
HSF1
LTR
LTR
HIV transcription
Nuclear
CD4+ T cell